

# Observation of Flame Propagation in a Premixed-Spray Stagnation Flow

Hiroyasu SAITOH, Shohji TSUSHIMA, Masaaki NEGORO,  
Fumiteru AKAMATSU and Masashi KATSUKI

Osaka University  
Department of Mechanical Engineering  
2-1 Yamada-oka, Suita, Osaka 565-0871, JAPAN

## ABSTRACT

Simultaneous application of Laser tomography and local chemiluminescence measurement to a premixed-spray flame stabilized in a stagnation flow have been made in order to investigate interrelation between spray characteristics and flame propagation behaviour, especially, influences of spatial and temporal nonuniformity of spray characteristics on flame propagation. Droplets and flame-front movements in a small area were monitored simultaneously. Time-series planar images of fuel droplets were processed and relative diameter of droplets were calculated based on Mie-scattering theory, and then the result was compared with PDA data to obtain 2-D spray characteristics. As a result, it was observed that dense spray region prevented flame from propagating, which changed the shape and location of vaporization zone. The speed and direction of flame propagation was affected by the spray characteristics, such as droplet diameter, number density and so on.

## 1. INTRODUCTION

Spray combustion is influenced by lots of parameters, such as evaporation, phase-interaction, size-distribution and number density of droplets and so on. In addition to such complexity, spray flows inherently feature inhomogeneity in space and time.

To observe the quantities in spray flames, therefore, advanced optical measurement techniques with sufficient spatial and temporal resolution must be developed and applied.

In our previous works [1-3], we extensively examined a premixed-spray flame by non-intrusive measurement techniques. As a result, it was revealed that both diffusion combustion mode (combustion of droplet clusters) and premixed-like combustion mode (flame propagation in a premixed-spray stream) coexist in the premixed-spray flame. In addition to the fact, it was confirmed that some portions of the premixed fuel spray stream disappeared rapidly due to flame propagation going through easy-to-burn regions, which we called “*preferential flame propagation* [3]”. However, influences of spray characteristics on flame propagation processes and its driving mechanism were not well studied because the detailed structure of the flame is hard to observe by macroscopic measurements used in the past.

In recent years, some researchers have tried to use counter-flow spray flame in order to investigate detailed structure of flame-front and flame propagating in a spray stream experimentally and theoretically [4-7]. Many of them used PDA (Phase Doppler Anemometry) or LDV (Laser Doppler Velocimeter) to obtain local characteristics of droplets. It seems essential for clarification of the flame structure to obtain at least time-series 2-D spray characteristics in a spray flame, such as droplet diameter, spatial distribution, velocity and so on.

In the present work, we intended to observe “flame propagation in a spray stream”, which is a specialty of spray combustion. In order to examine the influences of spatial and temporal non-uniformity of spray characteristics on flame propagation, both high-speed laser tomography for visualizing droplets and detection of chemiluminescence from radicals in the flame with MICRO system [8] were applied simultaneously to a premixed-spray flame stabilized in a stagnation flow. We also processed time-series planar images of visualized droplets to calculate droplet diameter and number density in an attempt to discuss influences of spray characteristics on propagating speed of a premixed-spray flame.

## 2. EXPERIMENTAL APPARATUS

The burner configuration is illustrated in Fig. 1 and the experimental apparatus used in this study is shown in Fig. 2. Liquid fuel of kerosene was atomized with a pressure nozzle placed at 650 mm upstream from the burner port. The spray was mixed with combustion air and issued upward from the inner burner port (35.6 mm i.d.) as a premixed-spray stream. A stagnation plate was placed at 50 mm above the burner port, whose temperature was kept constant (about 100 degrees centigrade) by cooling water. Coordinates  $h$  and  $r$  denote axial and radial distance measured from the center of the port, respectively. Kerosene-to-air mass ratio in the main flow was kept at  $0.045 \text{ kg}_{\text{fuel}}/\text{kg}_{\text{air}}$  corresponding to equivalence ratio of 0.75. The bulk velocity of the main flow was regulated at 1.33 m/s.

A typical image of the flame stabilized in the stagnation flow is presented in Fig. 3. Spray was visualized with an Ar-ion laser light sheet. Small fluctuations of the flame front in the vicinity of  $h = 38 \text{ mm}$  was observed. Since we confirmed that a calm flat-flame was formed with gaseous fuel under the same flow conditions in the preliminary experiment, the fluctuations of the flame front of spray flames can be mainly ascribed to the spatial and

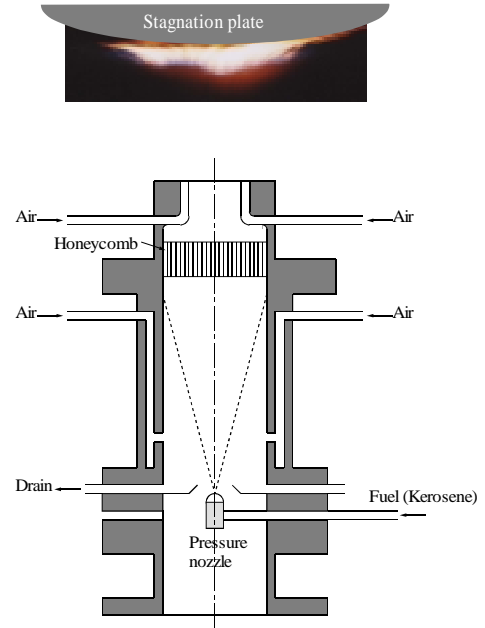


Fig. 1 Configuration of the premixed-spray flame Burner.

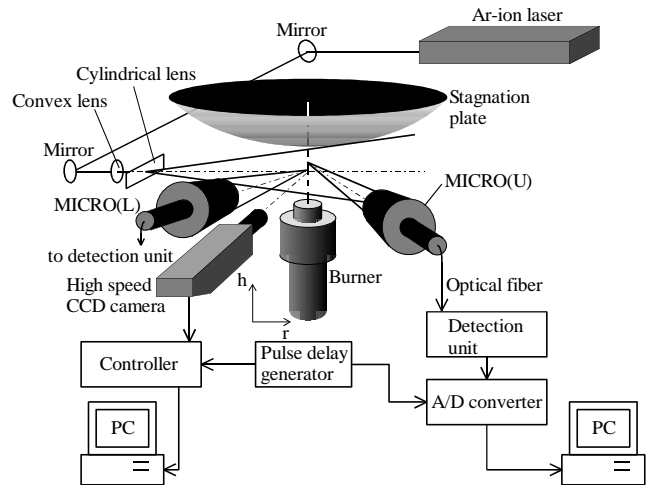


Fig. 2 Experimental apparatus.

temporal non-uniformity of the spray entering the flame region.

In order to correlate the local spray characteristics and the flame propagation behaviour, laser tomography and local chemiluminescence measurement were applied simultaneously to the

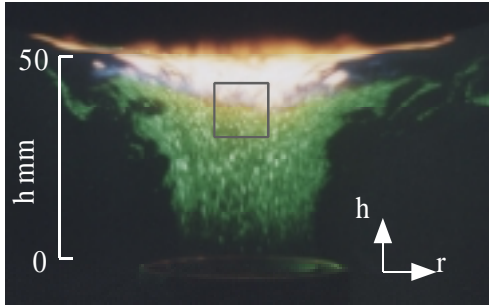


Fig. 3 Photograph of the flame where visualized spray stream is superimposed.

spray flame. Ar-ion laser (Spectra Physics, Stable 2017, wavelength: 514.5 nm) was used as a light source of Mie-scattering. The laser light was shaped into a vertical sheet by a series of lenses. Scattered lights from illuminated droplets within the small area indicated by a box in Fig. 3 were focused onto a CCD array ( $256 \times 256$  pixels) of a high-speed digital camera (Kodak, Ektapro HS4540) through an optical interference filter (peak wavelength: 514.5 nm, half width: 1.8 nm). The imaged area corresponds  $13.5\text{mm} \times 13.0\text{mm}$  and the frame rate was 1,125 fps.

In order to detect the movement of flame-front, OH chemiluminescence at two axial locations,  $h = 38$  mm and 41 mm, was detected by receiving optics named MICRO (Multi-color Integrated Cassegrain Receiving Optics) having an excellent spatial resolution [8]. MICRO has no chromatic aberration and minimized spherical aberration, because it consists of an optimized pair of concave and convex mirrors (see Fig. 4). Moreover, it has quite small effective control volume of 1.6 mm long and 200  $\mu\text{m}$  in diameter according to calculation of collection efficiency using a ray-tracing method. So the optics can collect emissions from a small region compared with lense optics.

The OH emission collected by the optics was detected by photomultiplier after removing background noise by an interference filter (peak wavelength: 308.5 nm, half width: 18.0 nm), and then digitized into 12 bit with an A/D converter, whose sampling rate was 50 kHz.

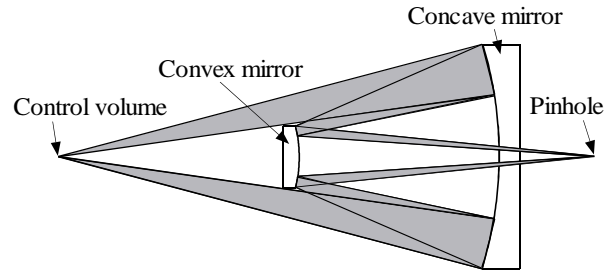


Fig. 4 Configuration of the MICRO system.

The timing of the A/D converter and the high-speed CCD camera was controlled by TTL signal from a pulse-delay generator (Stanford Research Systems, WC Model DG535).

### 3. RESULTS AND DISCUSSION

#### 3.1. 2-D spray characteristics measurement

Notwithstanding of the usefulness of PDA as a tool for droplet measurement, independent data by PDA are not sufficient in elucidation of detailed structure of spray flames. The main reasons are as follows,

- (1) Although it is necessary to observe spatial distribution of fuel droplets in clarification of spray flames, PDA data provide only local information of individual droplet at the measuring spot.
- (2) It is impossible to follow a history of each droplet by PDA.

In the present work, PDA data was used only in calibration of the relative mean diameter obtained by image processing with the absolute value.

Figure 5 shows a raw image of visualized droplets by laser tomography. The image (b), shown in the right side of the raw image (a), is an enlarged image of a droplet in the area indicated by a white box. The shape of the droplet is not a circle but distorted due to lack of pixel density. Therefore, it is not easy to determine the droplet center, i.e. the

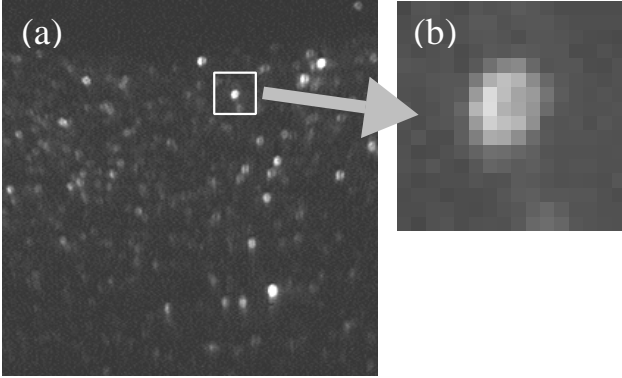


Fig. 5 Raw image of visualized droplets.

location of the droplet, and diameter directly from the raw droplet image.

Figure 6 demonstrates an example of image processing procedure used in this study. A source image obtained by laser tomography is presented in Fig. 6 (a). Firstly, Laplacian filter was applied to emphasize the edge of visualized droplets as shown in Fig. 6 (b). Then, the location of each droplet center is determined as demonstrated in Fig. 6 (c). From this image, spatial distribution of droplets can be obtained.

Mie-scattering theory [9] was applied in the calculation of droplet diameter. According to the theory, if the size parameter  $\alpha$  ( $= \pi D_p / \lambda$ ,  $D_p$ : droplet diameter,  $\lambda$ : wavelength of laser) is greater than 30, Mie scattering intensity,  $I_{MS}$ , increases in proportion to  $\alpha^2$ . The wavelength of laser used in the present study,  $\lambda$ , was 514.5 nm, and thus, the theory can be applied to the droplet diameter of greater than 4.9  $\mu\text{m}$ . Figure 7 shows the size distribution measured by PDA on the center axis in the non-combusting flow. Since all of droplets are larger than 4.9  $\mu\text{m}$ , we concluded that the estimation of diameter based on the Mie-scattering theory is acceptable. First, the area occupied by each droplet

was determined from the Laplacian filtered image. Secondly, the summation of pixel intensities in the area was calculated. The square root of the summation represents the relative value of diameter.

The calibration curve on the relationship between the absolute droplet diameter and Mie-scattering intensity was obtained in comparison with the size distribution measured by PDA. As a result, relative diameters were converted into absolute values. Figure 6 (d) shows the spatial distribution of droplets with the calculated diameter, although droplet diameters in the figure are depicted in a magnified scale.

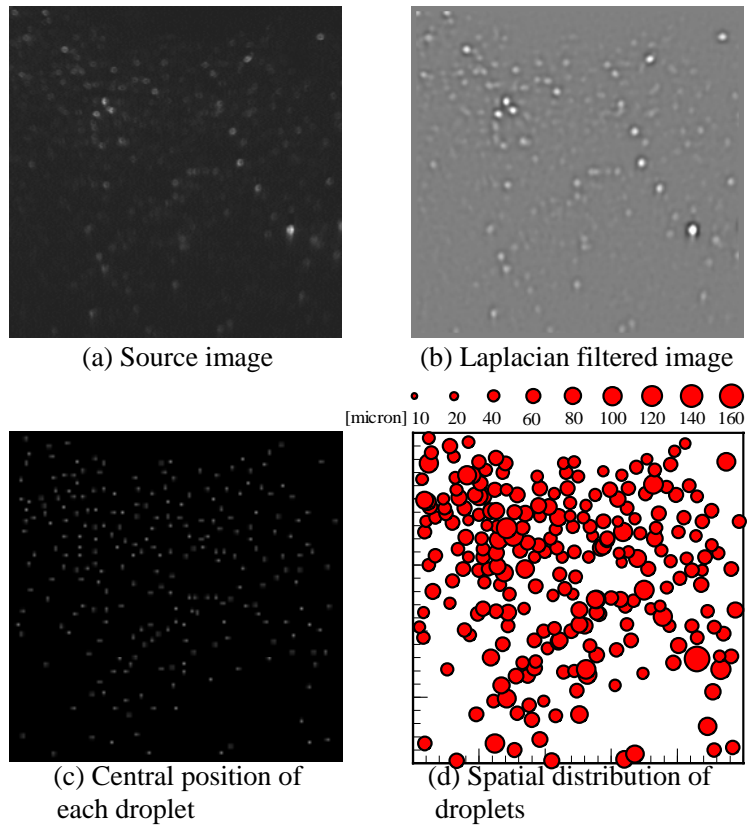


Fig. 6 Image process.

### 3.2. Time-series behaviours of droplets and propagating flame

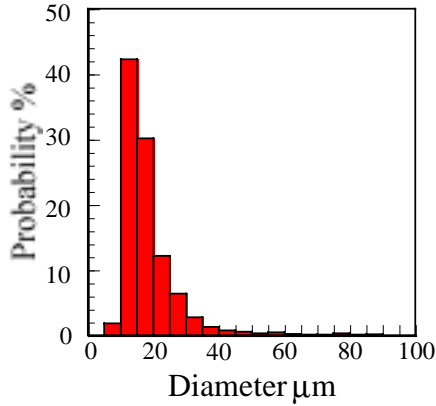


Fig. 7 Size distribution of premixed-spray measured by PDA at  $r=0$ ,  $h=10$  mm.

Time-series droplet behaviours and signal intensities of OH chemiluminescence detected at slightly separated two locations are shown in Fig. 8. At  $t = 168$  ms, the upper MICRO (U), which was placed 3 mm above the lower MICRO (L), detected an intense emission from OH radicals. This means the passage of flame through the focal point of MICRO (U). At about  $t = 170$  ms (2 ms later than the aforementioned instant), the lower MICRO (L) detected the flame front. This fact indicates that the flame moved downward against the flow, that is, the propagation speed at the point was increased. Therefore, we can understand that movement of the flame front in this spray burner is interpreted as the

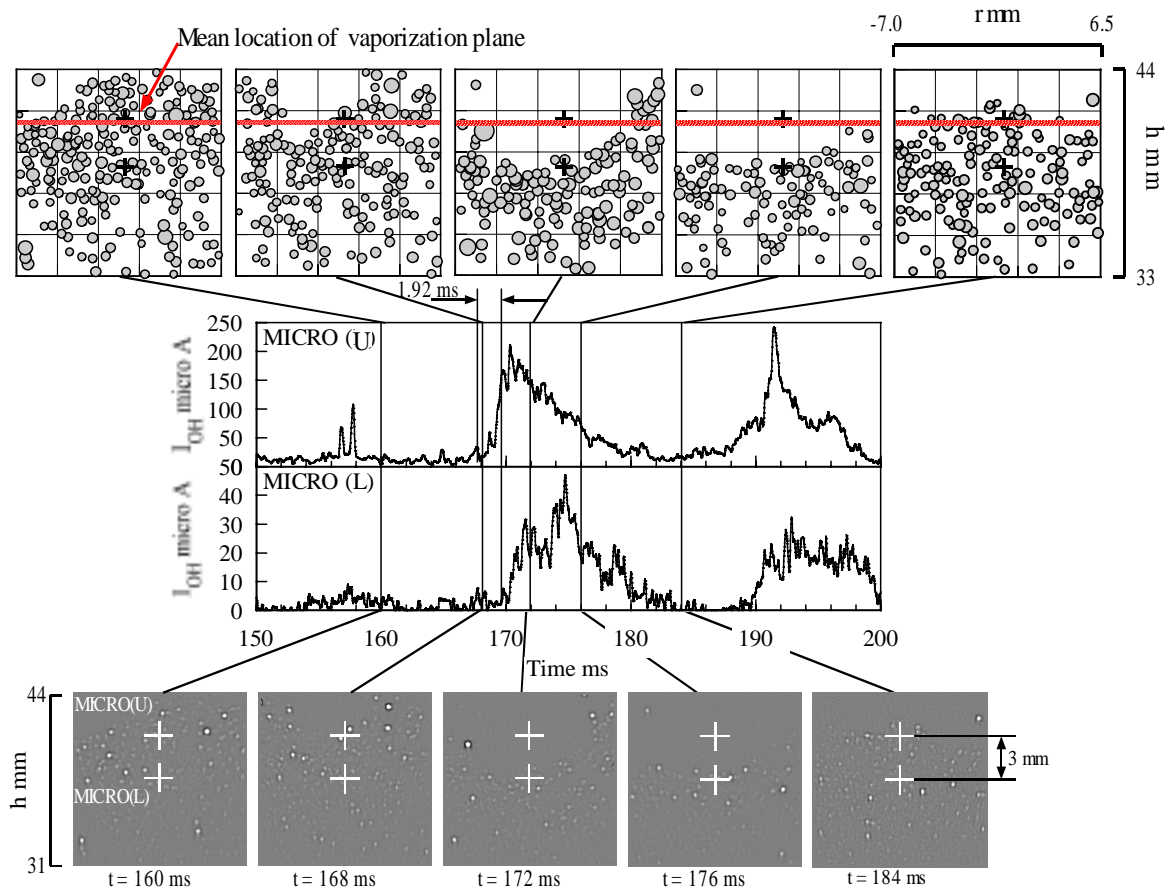


Fig. 8 Time-series droplet behaviours and signals of OH emission monitored at two different locations.

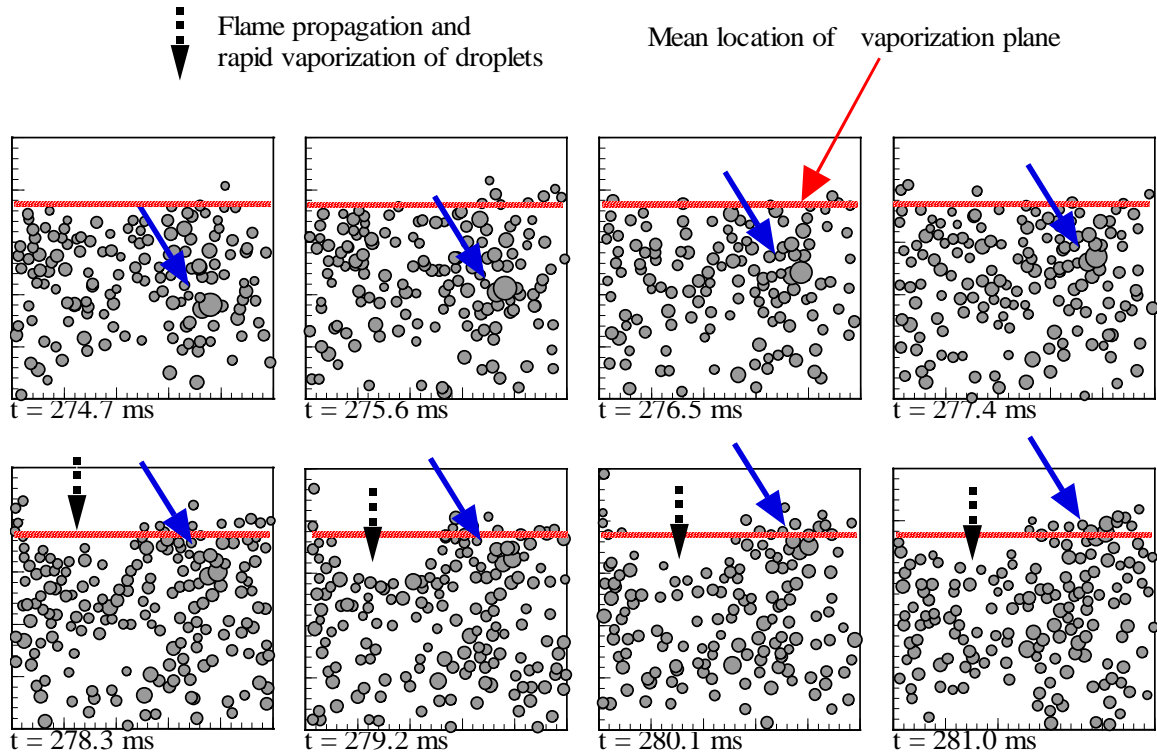


Fig. 9 Influences of spray characteristics on flame propagation process.

variation of flame propagation speed in the spray stream because the fluctuating axial component of gas-phase velocity in the premixed-spray stream leaving the burner port was less than 0.1 m/s.

In addition to the fact mentioned above, we observed that the boundary of spray region was deformed by flame propagation processes. Figure 9 shows the time variation of droplet movements monitored at the time-averaged position of flame-front. In a series of presented images, we can recognize that a portion of spray stream rapidly disappeared due to flame propagation into spray region as indicated by the dashed arrows. In contrast, a relatively dense portion of spray pointed by solid arrows survives long and makes the spray boundary protruding upwards out of the time averaged position of flame-front. We believe that the number density of droplet is one of the most influential factors to determine flame propagation speed in spray flow.

#### 4. CONCLUSIONS

The influences of spatial and temporal non-uniformity of spray characteristics on flame propagation process were studied by simultaneous application of laser tomography with high-speed CCD camera and detection of local OH chemiluminescence by MICRO system to the premixed-spray flame stabilized in a stagnation flow. The time-series planar images were processed and spatial distribution of spray and diameter of droplets based on Mie-scattering theory were calculated.

It was confirmed that the variations of shape and location of spray boundary were changed by the non-uniformity of spray characteristics, and that the number density of droplets was one of the influential factors on spray-flame propagation.

## 5. REFERENCES

- [1] Akamatsu, F., Mizutani, Y., Katsuki, M., Tsushima, S., Cho, Y.D. and Nakabe, K., Group Combustion Behavior of Droplets in a Premixed-spray Flame, Atomization and Sprays, Vol. 7, pp. 199-218, 1997.
- [2] Akamatsu, F., Mizutani, Y., Katsuki, M., Tsushima, S. and Cho, Y.D., Measurement of the Local Group Combustion Number of Droplet Clusters in a Premixed Spray Stream, Proceedings of the Combustion Institute, Vol. 24, pp. 1723-1729, 1996.
- [3] Tsushima, S., Saitoh, H., Akamatsu, F. and Katsuki, M., Observation of Combustion Characteristics of Droplet Clusters in a Premixed-spray Flame by Simultaneous Monitoring of Planar Spray Image and Local Chemiluminescence, Proceedings of the Combustion Institute, Vol. 27, pp. 1967-1974, 1998.
- [4] Chen, Z.H., Lin, T.H. and Sohrab, S.H., Combustion of Liquid Fuel Sprays in Stagnation-Point Flow, Combust. Sci. and Tech., Vol. 60, pp. 63-77, 1988.
- [5] Li, S.C., Libby, P.A. and Williams, F.A., Experimental and Theoretical Studies of Counterflow Spray Diffusion Flames, Proceedings of the Combustion Institute, Vol. 24, pp. 1503-1512, 1992.
- [6] Lacas, F., Darabiha, N., Versaevel, P., Rolon, J.C. and Candel, S., Influence of Droplet Number Density on the Structure of Strained Laminar Spray Flames, Proceedings of the Combustion Institute, Vol. 24, pp. 1523-1529, 1992.
- [7] Chen, G. and Gomez, A, Counterflow Diffusion Flames of Quasi-Monodisperse Electrostatic Sprays, Proceedings of the Combustion Institute, Vol. 24, pp. 1531-1539, 1992.
- [8] Akamatsu, F., Wakabayashi, T., Tsushima, S., Katsuki, M., Mizutani, Y., Ikeda, Y., Kawahara, N. and Nakajima, T., The Development of a Light-collecting Probe with High Spatial Resolution Applicable to Randomly Fluctuating Combustion Fields, Meas. Sci. Tech., Vol. 10, pp. 1240-1246, 1999.
- [9] Grehan, G. and Gouesbet, G., Mie Theory Calculations: New Progress, with Emphasis on Particle Sizing, Applied Optics, Vol. 18, No. 20, pp.3489-3493, 1979.